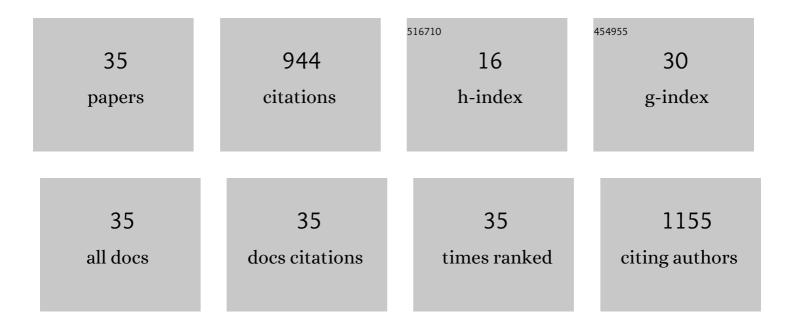
Gregor žerjav

List of Publications by Year in descending order

Source: https://exaly.com/author-pdf/6670992/publications.pdf Version: 2024-02-01



#	Article	IF	CITATIONS
1	Azine- and imine-linked conjugated polyHIPEs through Schiff-base condensation reaction. Polymer Chemistry, 2022, 13, 474-478.	3.9	8
2	Effect of Au loading on Schottky barrier height in TiO2Â+ÂAu plasmonic photocatalysts. Applied Surface Science, 2022, 579, 152196.	6.1	26
3	The influence of synthesis conditions on the visible-light triggered photocatalytic activity of g-C3N4/TiO2 composites used in AOPs. Journal of Environmental Chemical Engineering, 2022, 10, 107656.	6.7	15
4	Brookite vs. rutile vs. anatase: What`s behind their various photocatalytic activities?. Journal of Environmental Chemical Engineering, 2022, 10, 107722.	6.7	52
5	TiO2-β-Bi2O3 junction as a leverage for the visible-light activity of TiO2 based catalyst used for environmental applications. Catalysis Today, 2021, 361, 165-175.	4.4	23
6	Tunable poly(aryleneethynylene) networks prepared by emulsion templating for visible-light-driven photocatalysis. Catalysis Today, 2021, 361, 146-151.	4.4	9
7	Catalytic ozonation of an azo-dye using a natural aluminosilicate. Catalysis Today, 2021, 361, 24-29.	4.4	16
8	Evaluation of low-cost geo-adsorbents for As(V) removal. Environmental Technology and Innovation, 2021, 21, 101341.	6.1	4
9	The influence of Schottky barrier height onto visible-light triggered photocatalytic activity of TiO2Â+ÂAu composites. Applied Surface Science, 2021, 543, 148799.	6.1	22
10	Photocatalytic degradation of imidacloprid in the flat-plate photoreactor under UVA and simulated solar irradiance conditions—The influence of operating conditions, kinetics and degradation pathway. Journal of Environmental Chemical Engineering, 2021, 9, 105611.	6.7	29
11	Highly Porous Poly(arylene cyano-vinylene) Beads Derived through the Knoevenagel Condensation of the Oil-in-Oil Double Emulsion Templates. ACS Macro Letters, 2021, 10, 1248-1253.	4.8	8
12	Nanostructured composites based on Bi and Ti mixed oxides for visible-light assisted heterogeneous photocatalysis. , 2021, , 397-407.		0
13	Exploring the effect of morphology and surface properties of nanoshaped Pd/CeO2 catalysts on CO2 hydrogenation to methanol. Applied Catalysis A: General, 2021, 627, 118394.	4.3	22
14	Sputtered vs. sol-gel TiO2-doped films: Characterization and assessment of aqueous bisphenol A oxidation under UV and visible light radiation. Catalysis Today, 2020, 357, 380-391.	4.4	15
15	Influence of TiO2 Morphology and Crystallinity on Visible-Light Photocatalytic Activity of TiO2-Bi2O3 Composite in AOPs. Catalysts, 2020, 10, 395.	3.5	7
16	Revisiting terephthalic acid and coumarin as probes for photoluminescent determination of hydroxyl radical formation rate in heterogeneous photocatalysis. Applied Catalysis A: General, 2020, 598, 117566.	4.3	63
17	Effect of Surface Chemistry and Crystallographic Parameters of TiO2 Anatase Nanocrystals on Photocatalytic Degradation of Bisphenol A. Catalysts, 2019, 9, 447.	3.5	8
18	Hierarchically structured TiO2-based composites for Fenton-type oxidation processes. Journal of Environmental Management, 2019, 236, 591-602.	7.8	7

#	Article	IF	CITATIONS
19	Synthesis and adsorption behavior of mesoporous alumina and Fe-doped alumina for the removal of dominant arsenic species in contaminated waters. Journal of Environmental Chemical Engineering, 2019, 7, 102901.	6.7	50
20	TiO2-Bi2O3/(BiO)2CO3-reduced graphene oxide composite as an effective visible light photocatalyst for degradation of aqueous bisphenol A solutions. Catalysis Today, 2018, 315, 237-246.	4.4	35
21	Screening of catalytic activity of natural iron-bearing materials towards the Catalytic Wet Peroxide Oxidation of Orange II. Journal of Environmental Chemical Engineering, 2018, 6, 2027-2040.	6.7	13
22	Catalytic wet air oxidation of bisphenol A aqueous solution in trickle-bed reactor over single TiO2 polymorphs and their mixtures. Journal of Environmental Chemical Engineering, 2018, 6, 2148-2158.	6.7	12
23	Alkali and earth alkali modified CuOx/SiO2 catalysts for propylene partial oxidation: What determines the selectivity?. Applied Catalysis B: Environmental, 2018, 237, 214-227.	20.2	32
24	Influence of temperature and different hydroxides on properties of activated carbon prepared from saccharose. Characterization, thermal degradation kinetic and dyes removal from water solutions. Science of Sintering, 2018, 50, 255-273.	1.4	3
25	Characterization of selfâ€assembled layers made with stearic acid, benzotriazole, or 2â€mercaptobenzimidazole on surface of copper for corrosion protection in simulated urban rain. Materials and Corrosion - Werkstoffe Und Korrosion, 2017, 68, 30-41.	1.5	16
26	Electron trapping energy states of TiO 2 –WO 3 composites and their influence on photocatalytic degradation of bisphenol A. Applied Catalysis B: Environmental, 2017, 209, 273-284.	20.2	59
27	Improved electron–hole separation and migration in anatase TiO ₂ nanorod/reduced graphene oxide composites and their influence on photocatalytic performance. Nanoscale, 2017, 9, 4578-4592.	5.6	81
28	Modified diatomites for Fenton-like oxidation of phenol. Microporous and Mesoporous Materials, 2017, 239, 396-408.	4.4	29
29	Corrosion protection of brasses and zinc in simulated urban rain. Part II. The combination of inhibitors benzotriazole and 2â€mercaptobenzimidazole with stearic acid. Materials and Corrosion - Werkstoffe Und Korrosion, 2016, 67, 92-103.	1.5	12
30	Corrosion protection of brasses and zinc in simulated urban rain. Materials and Corrosion - Werkstoffe Und Korrosion, 2015, 66, 1402-1413.	1.5	7
31	Protection of copper against corrosion in simulated urban rain by the combined action of benzotriazole, 2-mercaptobenzimidazole and stearic acid. Corrosion Science, 2015, 98, 180-191.	6.6	74
32	Corrosion resistance of high-level-hydrophobic layers in combination with Vitamin E – (α-tocopherol) as green inhibitor. Corrosion Science, 2015, 97, 7-16.	6.6	66
33	Quaternary Ti–20Nb–10Zr–5Ta alloy during immersion in simulated physiological solutions: formation of layers, dissolution and biocompatibility. Journal of Materials Science: Materials in Medicine, 2014, 25, 1099-1114.	3.6	13
34	Structural Analysis, Electrochemical Behavior, and Biocompatibility of Novel Quaternary Titanium Alloy with near 1² Structure. Metallurgical and Materials Transactions A: Physical Metallurgy and Materials Science, 2014, 45, 3130-3143.	2.2	7
35	Electrochemical properties, chemical composition and thickness of passive film formed on novel Ti–20Nb–10Zr–5Ta alloy. Electrochimica Acta, 2013, 99, 176-189.	5.2	101